An essential role for SRC-activated STAT-3 in 14,15-EET–induced VEGF expression and angiogenesis

*Sergey Y. Cheranov,[1] *Manjula Karpurapu,[1] Dong Wang,[1] Baolin Zhang,[1] Richard C. Venema,[2] and Gadiparthi N. Rao[1]

[1]Department of Physiology, University of Tennessee Health Science Center, Memphis; and [2]Department of Pediatrics, Medical College of Georgia, Augusta

To understand the molecular mechanisms underlying 14,15-epoxyeicosatrienoic acid (14,15-EET)–induced angiogenesis, here we have studied the role of signal transducer and activator of transcription-3 (STAT-3). 14,15-EET stimulated the tyrosine phosphorylation of STAT-3 and its translocation from the cytoplasm to the nucleus in human dermal microvascular endothelial cells (HDMVECs). Adenovirus-mediated delivery of dominant negative STAT-3 substantially inhibited 14,15-EET–induced HDMVEC migration, and tube formation and Matrigel plug angiogenesis. 14,15-EET activated Src, as measured by its tyrosine phosphorylation and blockade of its activation by adenovirus-mediated expression of its dominant negative mutant, significantly attenuated 14,15-EET–induced STAT-3 phosphorylation in HDMVECs and the migration and tube formation of these cells and Matrigel plug angiogenesis. 14,15-EET induced the expression of vascular endothelial cell growth factor (VEGF) in a time- and Src-STAT-3–dependent manner in HDMVECs. Transfac analysis of VEGF promoter revealed the presence of STAT-binding elements and 14,15-EET induced STAT-3 binding to this promoter in vivo, and this interaction was inhibited by suppression of Src-STAT-3 signaling. Neutralizing anti-VEGF antibodies completely blocked 14,15-EET–induced HDMVEC migration and tube formation and Matrigel plug angiogenesis. These results reveal that Src-dependent STAT-3–mediated VEGF expression is a major mechanism of 14,15-EET–induced angiogenesis. (Blood. 2008;111:5581-5591)

Introduction

Cytochrome P450 epoxygenases (CYPs) such as CYP2C8/9 and CYP2J2 convert arachidonic acid to 4 EET regioisomers, namely 5,6-EET, 8,9-EET, 11,12-EET, and 14,15-EET.[1] A large body of data indicates that EETs play an important role in a wide variety of cellular functions including but not limited to hyperpolarization/vasodilation,[2,3] cell migration,[4] cell proliferation,[5,6] anti-inflammation,[7] and antiapoptosis.[8,9] Of notable interest among the cellular functions of EETs is their capacity to hyperpolarize vascular smooth muscle cells. However, their hyperpolarizing effects are limited due to their labile nature and conversion to dihydroxyeicosatrienoic acids (DHETs) by an enzyme, namely, soluble epoxide hydrolase (sEH).[10,11] Therefore, targeting sEH inhibition has been the focus of research in many laboratories to improve the stability of EETs and thereby their antihypertensive properties.[11,12]

In addition to their vasodilatory properties, many laboratories including ours have demonstrated that EETs stimulate angiogenesis.[13-15] Several studies have also demonstrated that stressors such as hypoxia induce the expression of CYP2C8/9, leading to increased production of EETs, perhaps as a protective response to stress in improving the blood supply.[16] EETs have also been reported to play a role in disease processes such as cancer metastasis.[17,18] Likewise, angiogenesis, besides its role in the embryonic development and wound healing, plays a role in disease processes such as atherosclerosis and cancer.[19-21] Therefore, to understand the relationship between EETs and angiogenesis and their involvement in the maintenance of vascular homeostasis versus disease processes, it is important to study the signaling mechanisms underlying the effects of EETs on new blood vessel formation.

Endothelial cell proliferation, migration, and differentiation play an important role in angiogenesis.[22] The Janus-activated kinase (Jak)–STAT signaling plays a role in the regulation of cell proliferation, migration, and survival.[23-25] Furthermore, many reports show that STAT-3 is preferentially involved in these cellular processes.[26-31] Besides, studies from our laboratory showed a role for STAT-3 in 15(S)-hydroxyeicosatetraenoic acid–induced angiogenesis.[32] The other signaling molecule that has been shown to play an important role in the regulation of cell proliferation, migration, and survival is Src.[33,34] In fact, a large body of evidence indicates that Src plays a crucial role in the regulation of angiogenesis and cancer.[35] Although the role of EETs as antihypertensive molecules has been well addressed[2,3] and the capacity of these molecules in stimulating angiogenesis has been demonstrated in recent years,[13-15] very little is known in regard to their mechanisms of intracellular signaling. In this study, we asked the question whether STATs and Src have any role in EET-induced angiogenesis. Here, we demonstrate for the first time that 14,15-EET, a CYP2C8/9 product of arachidonic acid, activates STAT-3 in human dermal microvascular endothelial cells (HDMVECs) in Src-dependent manner. Our findings also reveal that 14,15-EET–induced angiogenesis requires Src-STAT-3–dependent expression of VEGF.

Methods

Reagents

14,15-EET was bought from Cayman Chemicals (Ann Arbor, MI). Growth factor–reduced Matrigel was obtained from BD Biosciences (Bedford, MA). Phosphospecific anti–STAT-3 and anti-Src antibodies were bought from Cell Signaling Technology (Beverly, MA). Anti–STAT-3 and anti-Src antibodies were obtained from Upstate Biotechnology (Lake Placid, NY). Anti–β-tubulin (SC-9104), anti–STAT-3 (SC-482), and anti-VEGF (SC-152) antibodies and normal rabbit serum (SC-2338) were purchased from Santa Cruz Biotechnology (Santa Cruz, CA). Neutralizing anti-VEGF antibodies were bought from Chemicon International (Temecula, CA). Anti-CD31 antibodies were purchased from BD Pharmingen (Palo Alto, CA). Human VEGF enzyme-linked immunosorbent assay (ELISA) kit was obtained from Pierce (Rockford, IL). T4 polynucleotide kinase was procured from New England Biolabs (Ipswich, MA). [$\gamma^{32}P$]-ATP (3000 Ci/mmol) was bought from GE Healthcare (Piscataway, NJ). All the primers were made by IDT (Coralville, IA).

Adenoviral vectors

The construction of Ad-GFP, Ad-dnSTAT-3, and Ad-dnSrc was described previously.[31,36]

Cell culture

HDMVECs and human aortic smooth muscle cells (HASMCs) were bought from Cascade Biologics (Portland, OR). HDMVECs were grown in medium 131 containing microvascular growth supplements (MVGSs), 10 μg/mL gentamycin, and 0.25 μg/mL amphotericin B. In the case of HASMC growth, all the conditions were the same as for HDMVECs, except that medium 231 containing smooth muscle growth supplements was used. Cultures were maintained at 37°C in a humidified 95% air and 5% CO_2 atmosphere. HDMVECs and HASMCs were quiesced by incubating in medium 131 and 231, respectively, for 24 hours and used to perform the experiments unless otherwise indicated.

Cell migration assay

Cell migration was performed using a modified Boyden chamber method as described by Nagata et al.[37] The cell culture inserts containing membranes with 10 mm in diameter and 8.0-μm pore size (Nalge Nunc International, Rochester, NY) were placed in a 24-well tissue culture plate (Costar; Corning, Corning, NY). The lower surface of the porous membrane was coated with 70% Matrigel at 4°C overnight and then blocked with 0.1% heat-inactivated BSA at 37°C for 1 hour. HDMVECs were quiesced for 24 hours in medium 131, trypsinized, and neutralized with trypsin neutralizing solution. Cells were seeded into the upper chamber at 10^5 cells/well. Vehicle or 14,15-EET was added to the lower chamber at the indicated concentration. Both the upper and lower chambers contained medium 131. When the effect of dominant negative STAT-3 and Src mutants was tested on 14,15-EET–induced HDMVEC migration, cells were infected first with either Ad-GFP, Ad-dnSTAT-3, or Ad-Src at a multiplicity of infection (MOI) of 80 and quiesced before they were subjected to migration assay. In the case of testing the effect of neutralizing anti-VEGF antibodies on 14,15-EET–induced HDMVEC migration, cells were incubated with antibodies (3 μg/mL) for 30 minutes at 37°C and washed with medium 131. Cells were then seeded into each well, and wherever appropriate the antibodies were added to both the upper and lower chambers before the addition of 14,15-EET. After 6 hours of incubation at 37°C, nonmigrated cells were removed from the upper side of the membrane with cotton swabs, and the cells on the lower surface of the membrane were fixed in methanol for 15 minutes. The membrane was then stained with DAPI in vectashield mounting medium (Vector Laboratories, Burlingame, CA) and observed under Nikon diaphot fluorescence microscope with photometrics CH250 CCD camera (Nikon, Garden City, NY). Cells were counted in
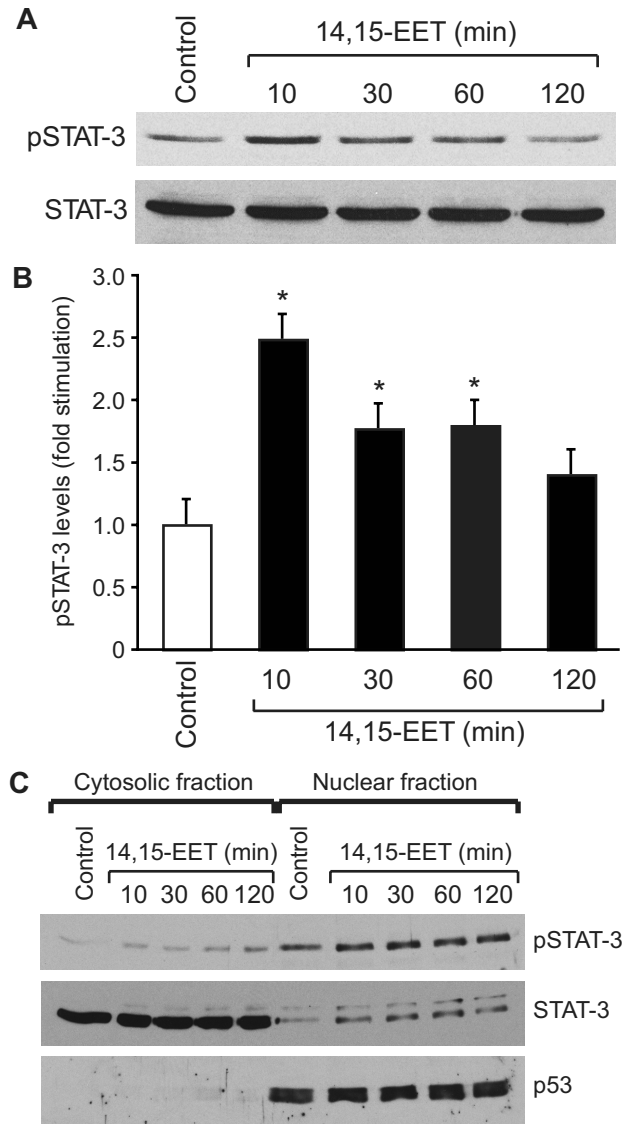
Figure 1. 14,15-EET activates STAT-3 in HDMVECs. Quiescent HDMVECs were treated with and without 14,15-EET (0.1 μM) for the indicated times and either cell extracts (A) or the cytoplasmic and nuclear factions (C) were prepared and analyzed by Western blotting for pSTAT-3 using its phosphospecific antibodies. (B) The bar graph represents the quantitative analysis of the time course effect of 14,15-EET on tyrosine phosphorylation of STAT-3 in triplicate. Error bars represent SD. The blot in panel A was reprobed with anti–STAT-3 antibodies for normalization. For testing the purity of the cytoplasmic and nuclear preparations, the blot in panel C was reprobed sequentially with anti–STAT-3 and anti-p53 antibodies. *$P < .01$ versus control.

5 randomly selected squares per well and presented as number of migrated cells per field.

Tube formation assay

Tube formation assay was performed as described by Nagata et al.[37] Twenty-four–well culture plates (Costar; Corning) were coated with growth factor–reduced Matrigel (BD Biosciences) in a total volume of 280 μL/well and allowed to solidify for 30 minutes at 37°C. HDMVECs were trypsinized, neutralized with TNS, and resuspended at 5×10^5/mL, and 200 μL of this cell suspension was added into each well. Vehicle or 14,15-EET, at the indicated concentration, was added to the appropriate well and the cells were incubated at 37°C for 6 hours. When the effect of dominant negative STAT-3 and Src mutants was tested on 14,15-EET–induced HDMVEC tube formation, cells were infected first with either Ad-GFP, Ad-dnSTAT-3, or Ad-Src at an MOI of 80 and quiesced before they were subjected to tube formation. In the case of testing the effect of

Figure 2. Adenovirus-mediated expression of dnSTAT-3 suppresses 14,15-EET–induced HDM-VEC migration and tube formation in vitro and Matrigel plug angiogenesis in vivo. (A,B) HDMVECs were transduced with Ad-GFP or Ad-dnSTAT-3 at an MOI of 80, quiesced, and subjected to 14,15-EET–induced migration (A,B) or tube formation (C,D). (E,F) C57BL/6 mice were injected subcutaneously with 0.5 mL Matrigel premixed with vehicle or 50 μM 14,15-EET with and without Ad-GFP or Ad-dnSTAT-3 (5×10^9 pfu/mL). One week later, the animals were killed and the Matrigel plugs were harvested from underneath the skin and either analyzed for hemoglobin content using Drabkin reagent or immunostained for CD31 expression using anti-CD31 antibodies. The values in the bar graphs in panels B, D, and E are the means plus or minus SD of 3 independent experiments or 4 animals. *$P < .01$ vs Ad-GFP; **$P < .01$ vs AD-GFP + 14,15-EET.
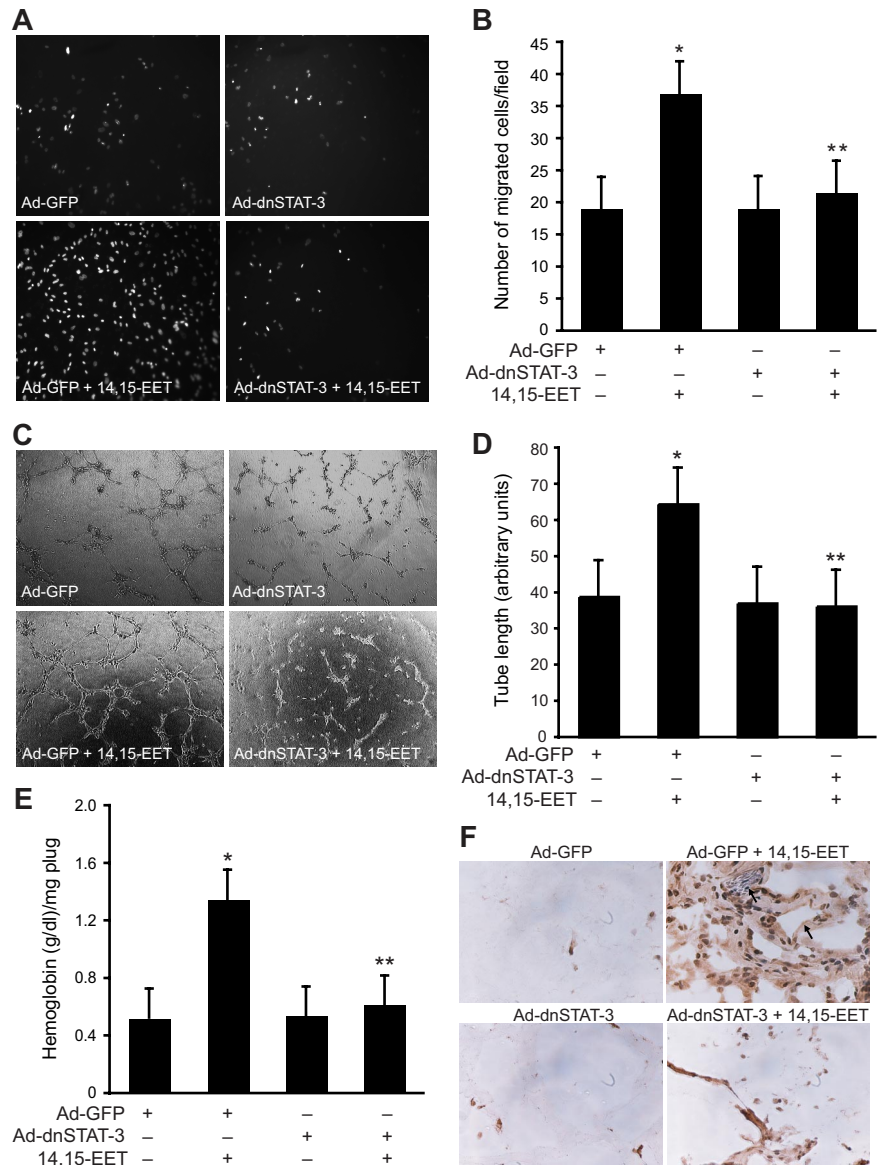
neutralizing anti-VEGF antibodies on 14,15-EET–induced HDMVEC tube formation, cells were incubated with antibodies (3 μg/mL) for 30 minutes at 37°C and washed with medium 131. Cells were then seeded into each well and wherever appropriate the antibodies were added to the well before the addition of 14,15-EET. Tube formation was observed under an inverted microscope (Eclipse TS100; Nikon, Tokyo, Japan). Images were captured with a CCD color camera (KP-D20AU; Hitachi, Ibaraki, Japan) attached to the microscope and tube length was measured using the National Institutes of Health (NIH) Image J (Bethesda, MD).

Western blot analysis

After appropriate treatments and rinsing with cold PBS, HDMVECs were lysed in 500 μL lysis buffer (PBS, 1% nonidet P-40, 0.5% sodium deoxycholate, 0.1% SDS, 100 μg/mL PMSF, 100 μg/mL aprotinin, 1 μg/mL leupeptin, and 1 mM sodium orthovanadate) and scraped into 1.5-mL Eppendorf tubes. After standing on ice for 20 minutes, the cell lysates were cleared by centrifugation at 12 000 rpm for 20 minutes at 4°C. Cell lysates containing equal amount of protein were resolved by electrophoresis on 0.1% SDS and 10% polyacrylamide gels. The proteins were transferred electrophoretically to a nitrocellulose membrane (Hybond; GE Healthcare). After blocking in 10 mM Tris-HCl buffer, pH 8.0, containing 150 mM sodium chloride, 0.1% Tween 20, and 5% (wt/vol) nonfat dry milk, the

membrane was treated with appropriate primary antibodies followed by incubation with horseradish peroxidase (HRP)–conjugated secondary antibodies. The antigen-antibody complexes were detected using chemiluminescence reagent kit (GE Healthcare).

RT-PCR

After appropriate treatments, total cellular RNA was isolated from HDM-VECs using Trizol reagent as per the manufacture's guidelines (Invitrogen, Carlsbad, CA). Reverse transcription was carried out with Superscript III First-Strand Synthesis System for reverse transcription–polymerase chain reaction (RT-PCR) based on supplier's protocol (Invitrogen). The cDNA was then used as template for PCR using specific primers for human VEGF (accession no. AF486837[38]; forward, 5′-TCTGCTGTCTTGGGTGCATT-3′; reverse, 5′-GCGAGTCTGTGTTTTTGCAG-3′), and human β-actin (accession no. NM 001101) (forward, 5′-AGCCATGTACGTTGCTAT-3′; reverse 5′-GATGTCCACGTCACACTTCA-3′). The amplification was carried out on a Gene Amp PCR System 2400 (Applied Biosystems, Foster City, CA), using the following conditions: for VEGF, 95°C for 5 minutes followed by 30 cycles at 95°C for 45 seconds, 56°C for 45 seconds, and 72°C for 55 seconds with final extension at 72°C for 7 minutes; for β-actin, 95°C for 5 minutes followed by 30 cycles at 95°C for 45 seconds, 55°C for 45 seconds, and 72°C for 50 seconds with final extension at 72°C for

7 minutes. The amplified RT-PCR products were separated on 1.2% (wt/vol) agarose or 8% native polyacrylamide gels, stained with ethidium bromide, pictures were captured using AlphaEase Digital Imaging System (Alpha Innotech, San Leandro, CA), and the band intensities were quantified using NIH Image J.

Electrophoretic mobility shift assay

After appropriate treatments, nuclear extracts were prepared from HDM-VECs as described previously.[32] The protein content of the nuclear extracts was determined using a Micro BCA Protein Assay Reagent Kit (Pierce). Protein-DNA complexes were formed by incubating 10 μg nuclear protein in a total volume of 20 μL consisting of 15 mM HEPES, pH 7.9, 3 mM Tris-HCl, pH 7.9, 60 mM KCl, 1 mM EDTA, 1 mM PMSF, 1 mM dithiothreitol, 2.5 μg/mL bovine serum albumin (BSA), 1 μg/mL poly (dI-dC), 15% glycerol, and 100 000 cpm [^{32}P]-labeled oligonucleotide probe for 30 minutes on ice. The protein-DNA complexes were resolved by electrophoresis on a 4% polyacrylamide gel using 1× Tris-glycine-EDTA buffer (25 mM Tris-HCl, pH 8.5, 200 mM glycine, 0.1 mM EDTA). Double-stranded oligonucleotides from −862 to −827 region of human VEGF promoter (accession no. AF095785) (5′-GCATCCCTGGACAC-TTCCCAAAGGACCCCAGTCACT-3′ and 3′-CGTAGGGACCTGTGA-AGGGTTTCCTGGGGTCAGTGA-5′) were used as [^{32}P]-labeled probes to measure STAT DNA-binding activities. Double-stranded oligonucleotides were labeled with [γ^{32}P]-ATP using the T4 polynucleotide kinase kit following the supplier's protocol.

Chromatin immunoprecipitation assay

Chromatin immunoprecipitation (ChIP) assay was performed on HDM-VECs using ChIP assay kit following supplier's protocol (Upstate Biotechnology). STAT-3-DNA complexes were immunoprecipitated using anti–STAT-3 antibody. Preimmune rabbit serum was used as a negative control. The immunoprecipitated DNA was un–cross-linked, subjected to Proteinase K digestion, and purified using QIAquick columns (Qiagen, Valencia, CA). The purified DNA was used as a template for PCR amplification using primers (forward, 5′-TTGGTGC-CAAATTCTTCTCC-3′; reverse, 5′-CACACGTCCTCACTCTCGAA-3′) flanking the putative STAT-binding sites located at −848 and −630 in human VEGF promoter region (accession no. AF095785). The PCR products were resolved on 1.2% agarose or 8% native polyacrylamide gels and stained with ethidium bromide, and the band intensities were quantified using NIH Image J.

Matrigel plug angiogenesis assay

Matrigel plug assay was performed essentially as described by Medhora et al.[13] C57BL/6 mice (8 weeks old) were lightly anesthetized with sodium pentobarbital (50 mg/kg, intraperitoneally) and were injected subcutaneously with 0.5 mL Matrigel that was premixed with vehicle or 50 μM 14,15-EET along the dorsal midline (due to its highly labile characteristic feature, one higher bolus dose of 14,15-EET was added to the Matrigel to facilitate its continuous availability over a period of several days). The injection was made rapidly with a B-D 26½G needle to ensure the entire content was delivered as a single plug. Wherever the effect of Ad-GFP (5×10^9 pfu/mL), Ad-dnSTAT-3 (5×10^9 pfu/mL), Ad-Src (5×10^9 pfu/mL), preimmune serum (3 mg/mL), or neutralizing anti-VEGF (3 mg/mL) antibodies was tested on 14,15-EET–induced angiogenesis, they were added to the Matrigel prior to injecting into mice. The mice were allowed to recover and 7 days later, unless otherwise stated, the animals were killed by inhalation of CO_2 and the Matrigel plugs were harvested from underneath the skin. The plugs were homogenized in 1 mL deionized H_2O on ice and cleared by centrifugation at 10 000 rpm for 6 minutes at 4°C. The supernatant was collected and used in duplicate to measure hemoglobin content with Drabkin reagent along with hemoglobin standard essentially according to the manufacturer's protocol (Sigma Chemical, St Louis, MO). The absorbance was read at 540 nm in an ELISA plate reader (Spectra Max 190; Molecular Devices, Sunnyvale, CA). These experiments were repeated
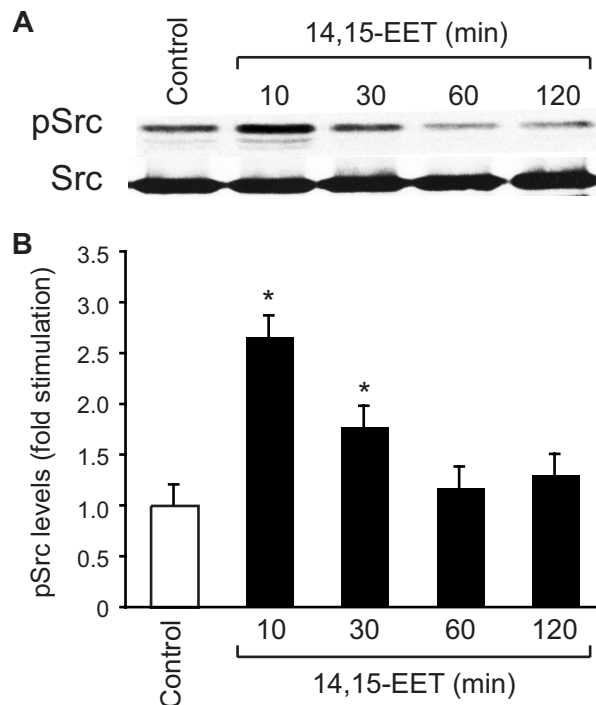
Figure 3. 14,15-EET activates Src in HDMVECs. (A) Quiescent HDMVECs were treated with and without 14,15-EET (0.1 μM) for the indicated times, and cell extracts were prepared and analyzed by Western blotting for pSrc using its phosphospecific antibodies. The blot was reprobed with anti-Src antibodies for normalization. (B) The bar graph represents the quantitative analysis of the time course effect of 14,15-EET on tyrosine phosphorylation of Src in triplicate. *$P < .01$ vs control. Error bars represent SD.

at least 3 times with 4 mice for each group and the values are expressed as grams per deciliter of hemoglobin per milligram plug.

Immunohistochemistry

After retrieving the Matrigel plugs from mice, they were snap-frozen in OCT compound. Cryosections (5 μm) were made using Leica Kryostat machine (CM3050S; Heidelberg, Germany) and stained with anti-CD31 antibody (1:500 dilution; BD Pharmingen), followed by sequential incubation with biotinylated anti–rat IgG (1:300 dilution), avidin-biotin peroxidase, and diaminobenzidine substrate (Vector Laboratories). The sections were counterstained with hematoxylin and examined under a light microscope (Eclipse 50i; Nikon, Tokyo, Japan) in 6 random fields (400× magnification) from each group. Images were captured using Nikon Digital Sight DS-L1 system.

VEGF ELISA

VEGF released into the culture media was measured using an ELISA kit following the manufacturer's instructions (Pierce).
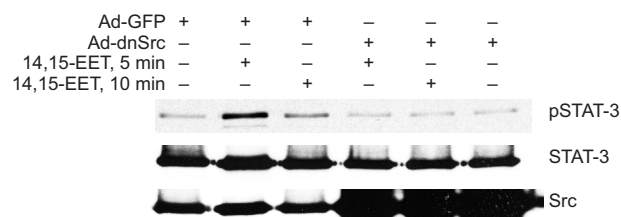
Figure 4. Adenovirus-mediated expression of dnSrc inhibits 14,15-EET–induced STAT-3 phosphorylation in HDMVECs. HDMVECs that were transduced with Ad-GFP or Ad-dnSrc at an MOI of 80 were treated with and without 14,15-EET (0.1 μM) for the indicated times, and cell extracts were prepared and analyzed by Western blotting for pSTAT-3 using its phosphospecific antibodies. The blot was reprobed sequentially with anti–STAT-3 antibodies for normalization and anti-Src antibodies for overexpression of Src.

Figure 5. Adenovirus-mediated expression of dnSrc suppresses 14,15-EET–induced HDMVEC migration and tube formation in vitro and Matrigel plug angiogenesis in vivo. (A,B) HDMVECs were transduced with Ad-GFP or Ad-dnSrc at an MOI of 80, quiesced, and subjected to 15(S)-HETE–induced migration (A,B) or tube formation (C,D). (E,F) C57BL/6 mice were injected subcutaneously with 0.5 mL Matrigel premixed with vehicle or 50 μM 14,15-EET with and without Ad-GFP or Ad-dnSrc (5 × 10^9 pfu/mL). One week later, the animals were killed and the Matrigel plugs were harvested from underneath the skin and analyzed for either hemoglobin content with Drabkin reagent or immunostained for CD31 expression using anti-CD31 antibodies. The values in the bar graphs in panels B, D, and E are the means plus or minus SD of 3 independent experiments or 4 animals. *$P <$ .01 vs Ad-GFP; **$P <$ .01 vs AD-GFP + 14,15-EET.
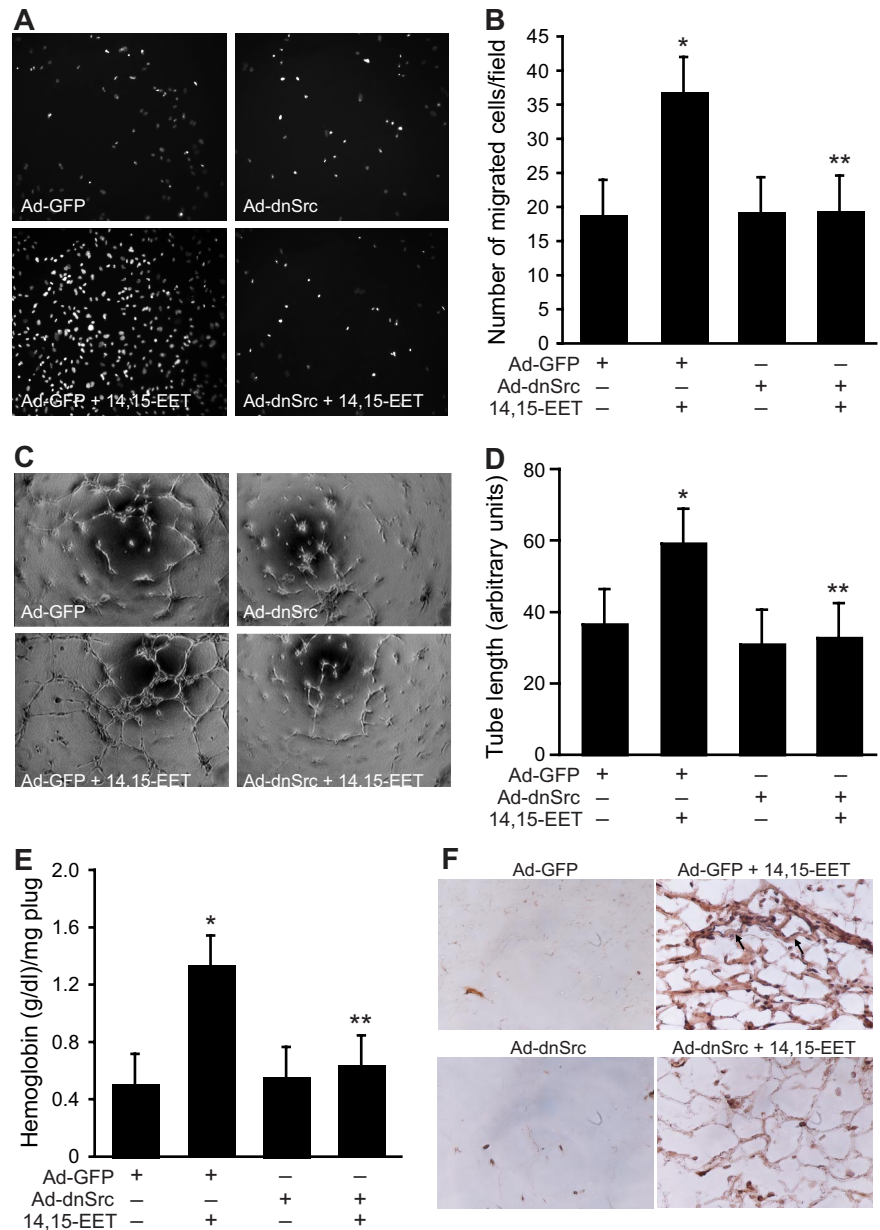
Statistics

All the experiments were repeated 3 times and data are presented as means plus or minus SD. The treatment effects were analyzed by Student t test, and the P values less than .05 were considered statistically significant. In the case of ChIP analysis, EMSA, and Western blotting, 1 representative set of data is shown.

Results

14,15-EET activates STAT-3 in HDMVECs

To understand the mechanisms of 14,15-EET–induced angiogenesis, we have studied the role of STAT-3. Quiescent HDMVECs were treated with and without 14,15-EET (0.1 μM) for the indicated times, and an equal amount of protein from control and each treatment was analyzed for phosphorylated STAT-3 using its phosphospecific antibodies. 14,15-EET stimulated tyrosine (Tyr705) phosphorylation of STAT-3 in a time-dependent manner, with a

maximum increase of 2.5-fold at 10 minutes and gradually declining thereafter reaching basal levels by 120 minutes (Figure 1A,B). Upon phosphorylation, STATs form homodimers or heterodimers with other members of their family and translocate from the cytoplasm to the nucleus where they bind to promoter regions and influence the gene transcription.[23] To study STAT-3 translocation, cells were treated with and without 14,15-EET (0.1 μM) for various time periods, and the cytoplasmic and nuclear extracts were prepared and analyzed for phosphorylated STAT-3 levels as described in "Western blot analysis." The major levels of phosphorylated STAT-3 were found in the nuclear fractions of both control and treated cells. In addition, the phosphorylated STAT-3 levels were found to be 2-fold higher in the nuclear fractions of 14,15-EET–treated cells compared with untreated cells (Figure 1C). To confirm the nuclear translocation of STAT-3, the blot was reprobed with anti-p53 antibodies. As expected, p53 was found only in the nuclear fractions, a result that confirms the purity of the cytoplasmic and nuclear preparations. Furthermore, sequential

reprobing of the membrane with anti–STAT-3 antibodies indicated that the majority of the total STAT-3 was present in the cytoplasm and only a small fraction of it was phosphorylated in response to 14,15-EET (Figure 1C).

### STAT-3 mediates 14,15-EET–induced HDMVEC migration, tube formation, and Matrigel plug angiogenesis

Next we tested the role of STAT-3 in 14,15-EET–induced HDM-VEC migration and tube formation. 14,15-EET stimulated HDM-VEC migration by approximately 2-fold as measured by modified Boyden chamber method, and adenovirus-mediated expression of dnSTAT-3 attenuated this effect (Figure 2A,B). Similarly, 14,15-EET induced HDMVEC tube formation by approximately 2-fold, and this effect was also found to be STAT-3 dependent as adenovirus-mediated expression of its dominant negative mutant inhibited this activity (Figure 2C,D). To obtain additional evidence for the role of STAT-3 in 14,15-EET–induced angiogenesis, we used Matrigel plug angiogenesis model. As shown in Figure 2E,F, 14,15-EET (50 μM) induced Matrigel plug angiogenesis and dnSTAT-3 significantly inhibited this effect.

14,15-EET–stimulated STAT-3 phosphorylation in HDMVECs and their migration, and tube formation and Matrigel plug angiogenesis are mediated by Src

In addition to Jak, a role for Src in the phosphorylation and activation of STAT-3 has been demonstrated in, at least, some cell types.[39,40] In this aspect, we have previously shown that 14,15-EET activates Src in HDMVECs.[15] To find whether Src mediates 14,15-EET–induced activation of STAT-3, we first studied a time course effect of this lipid molecule on tyrosine phosphorylation of Src. 14,15-EET induced the tyrosine (Tyr416) phosphorylation of Src in a time-dependent manner with a maximum 2.5-fold increase at 10 minutes and declining thereafter reaching basal levels by 60 minutes (Figure 3A,B). Next, we tested the effect of dnSrc on 14,15-EET–induced phosphorylation of STAT-3. Adenovirus-mediated expression of dnSrc without affecting the total STAT-3 levels completely inhibited its tyrosine phosphorylation induced by 14,15-EET (Figure 4). To confirm the role of Src in 14,15-EET–induced STAT-3–mediated angiogenic signaling events, we further tested the effect of dnSrc on HDMVEC migration, and tube formation and Matrigel plug angiogenesis. Adenovirus-mediated expression of dnSrc completely inhibited 14,15-EET–induced HDMVEC migration and tube formation (Figure 5A-D). In addition, adenovirus-mediated expression of dnSrc blocked 14,15-EET–induced Matrigel plug angiogenesis (Figure 5E,F).

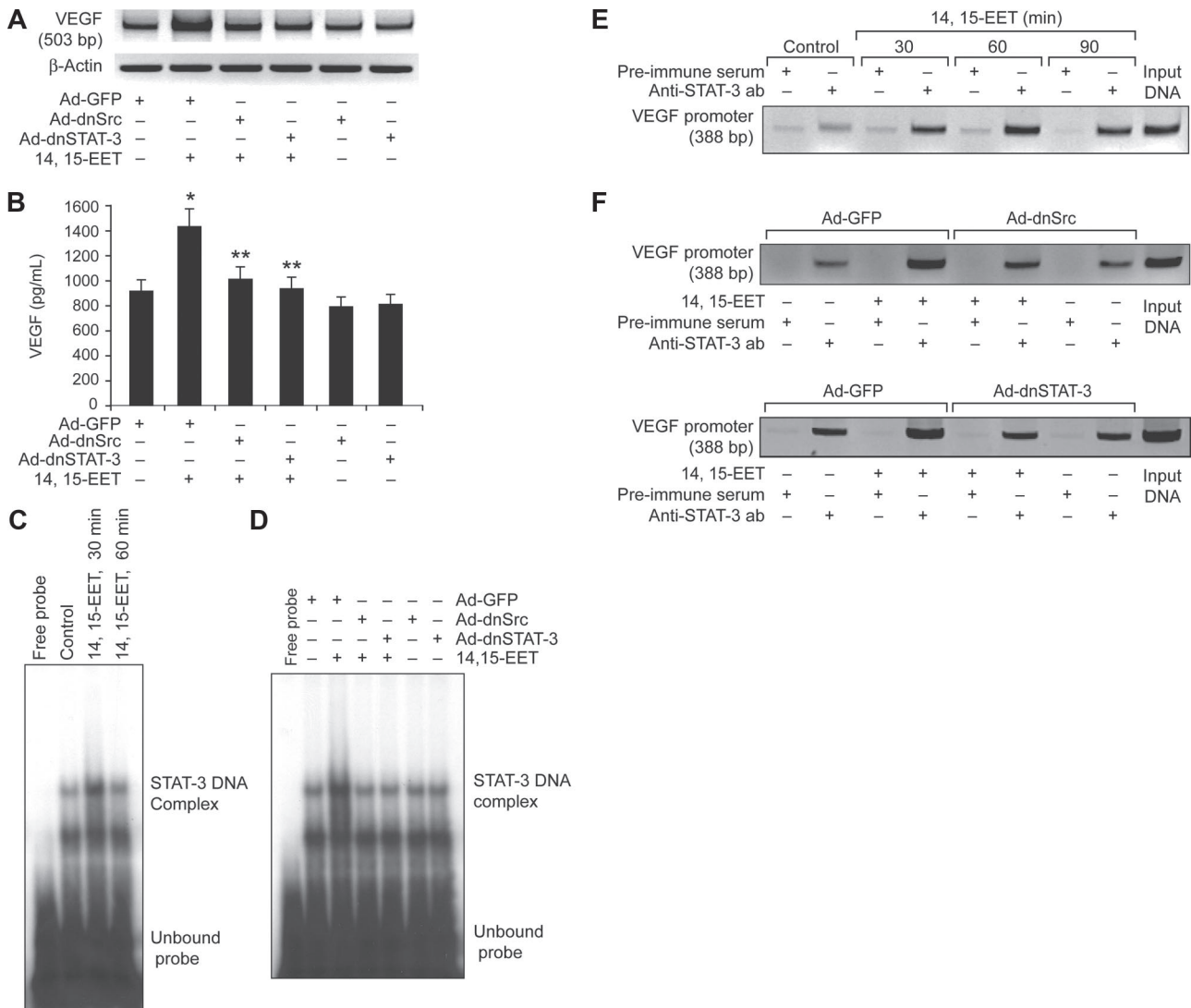### 14,15-EET induces VEGF expression in HDMVECs via activation of Src-STAT-3 signaling

It was reported that Src and STAT-3 mediate VEGF expression in response to some angiogenic stimulants.[41,42] To determine whether 14,15-EET induces the expression of VEGF, and if so, the role of Src and STAT-3, quiescent HDMVECs were treated with and without 14,15-EET (0.1 μM) for the indicated times, and either total cellular RNA was isolated or cell extracts were prepared. An equal amount of RNA from control and each treatment was then analyzed by RT-PCR for VEGF mRNA levels using its specific primers. 14,15-EET induced VEGF mRNA levels in a time-dependent manner with 5-fold increase at 4 hours (Figure 6A). To confirm this result, we next measured VEGF protein levels by Western blotting using its specific antibodies. As shown in Figure 6B, 14,15-EET induced the expression of VEGF in a time-
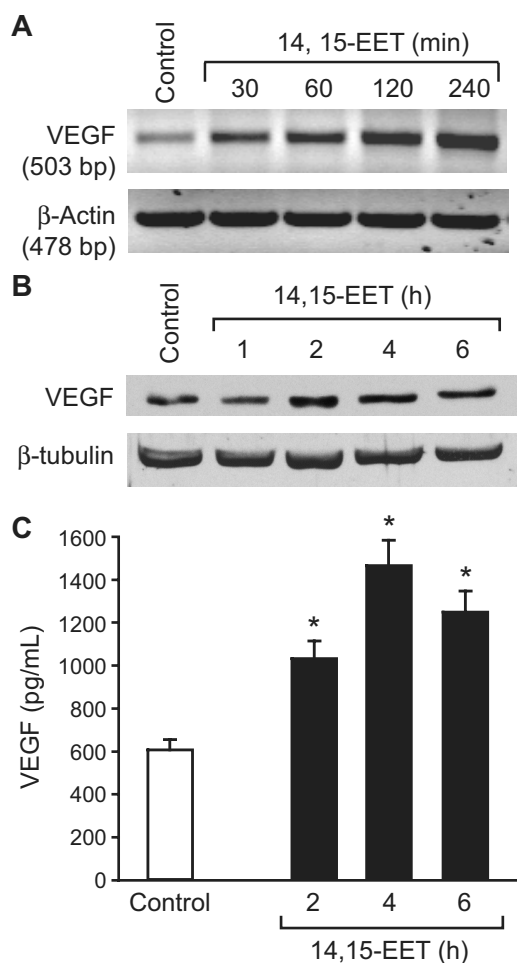
Figure 6. 14,15-EET induces VEGF expression in a time-dependent manner in HDMVECs. Quiescent HDMVECs were treated with and without 14,15-EET (0.1 μM) for the indicated time periods and either RNA was isolated and analyzed for VEGF mRNA levels by RT-PCR (A), cell extracts were prepared and analyzed for VEGF levels by Western blotting (B), or the culture medium was collected and assayed for released VEGF by ELISA (C). The values in the bar graph in panel C are the means plus or minus SD of 3 independent experiments. *$P < .01$ vs control.

dependent manner with a maximum 2-fold increase at 4 hours. Similarly, 14,15-EET induced the release of VEGF into the culture medium in a time-dependent manner with a maximum of 2-fold effect at 4 hours (Figure 6C). Blockade of Src and STAT-3 by adenovirus-mediated expression of their dominant negative mutants significantly blunted the 14,15-EET–induced VEGF expression at mRNA level (Figure 7A). Similarly, blockade of Src and STAT-3 by adenovirus-mediated expression of their dominant negative mutants inhibited 14,15-EET–induced VEGF release into the culture medium as measured by ELISA (Figure 7B). Transfac analysis of human VEGF promoter revealed the presence of a putative STAT-binding motif spanning from −848 to −841. To test whether STATs bind to this element in response to 14,14-EET, we first performed its time course effect using STAT consensus element present in the VEGF promoter as a [^{32}P]-labeled probe. 14,15-EET induced STAT DNA-binding activity with 2-fold increase at 30 minutes (Figure 7C). Blockade of Src-STAT-3 signaling by adenovirus-mediated expression of their dominant negative mutants completely inhibited 14,15-EET–induced STAT DNA-binding activity (Figure 7D). To obtain additional evidence for the role of STAT-3 in the regulation of VEGF, we measured STAT-3 binding to the promoter of VEGF in vivo using chromatin

Figure 7. 14,15-EET–induced VEGF expression is mediated by Src-STAT-3 signaling in HDMVECs. (A,B) HDMVECs were transduced with Ad-GFP, Ad-dnSrc, or Ad-dnSTAT-3 with an MOI of 80, quiesced, and treated with and without 14,15-EET (0.1 μM) for 2 hours, and RNA was isolated and analyzed for VEGF mRNA levels by RT-PCR (A), or for 6 hours, and the VEGF release into the culture medium was measured by ELISA (B). (C,E) Quiescent HDMVECs were treated with and without 14,15-EET (0.1 μM) for the indicated time periods and nuclear extracts were either prepared and analyzed by EMSA for STAT binding using [^{32}P]-labeled STAT consensus sequence of VEGF promoter as a probe in vitro (C) or processed for ChIP analysis of STAT-3 binding to VEGF promoter in vivo (E). (D,F) HDMVECs that were transduced with Ad-GFP, Ad-dnSrc, or Ad-dnSTAT-3 with an MOI of 80 and quiesced were treated with and without 14,15-EET (0.1 μM) either for 30 minutes and nuclear extracts were prepared and analyzed by EMSA for STAT binding as described in panel C (D) or for 1 hour and processed for ChIP analysis of STAT-3 binding to VEGF promoter in vivo (F). The values in the bar graph in panel B are the means plus or minus SD of 3 independent experiments. *$P <$ .01 vs Ad-GFP; **$P <$ .01 vs AD-GFP + 14,15-EET.

immunoprecipitation (ChIP) assay. ChIP analysis revealed a time-dependent binding of STAT-3 to VEGF promoter in vivo (Figure 7E). In addition, blockade of Src and STAT-3 via adenovirus-mediated expression of their dominant negative mutants suppressed the binding of STAT-3 to VEGF promoter in vivo (Figure 7F).

14,15-EET–induced HDMVEC migration and tube formation and Matrigel plug angiogenesis are mediated by VEGF

To test the role of VEGF in 14,15-EET–induced angiogenesis, we next studied the effect of neutralizing anti-VEGF antibodies on 14,15-EET–induced HDMVEC migration and tube formation. Addition of neutralizing anti-VEGF antibodies (3 μg/mL) completely suppressed 14,15-EET–induced HDMVEC migration and tube formation (Figure 8A-D). Neutralizing anti-VEGF antibodies also inhibited 14,15-EET–induced Matrigel plug angiogenesis (Figure 8E,F).

Lack of effect of 14,15-EET on VEGF induction in HASMCs

To understand the paracrine mechanisms in 14,15-EET–induced angiogenesis, we also tested its effects on VEGF expression in HASMCs. As shown in Figure 9A-C, 14,15-EET had no significant effect on induction of VEGF in HASMCs as determined by RT-PCR, Western blotting, and ELISA.

## Discussion

The important findings of the present study are as follows: (1) 14,15-EET stimulated the tyrosine phosphorylation of STAT-3 and its translocation from the cytoplasm to the nucleus. (2) Interference with activation of STAT-3 via adenovirus-mediated expression of its dominant negative mutant abolished 14,15-EET–induced HDMVEC migration, tube formation and Matrigel plug
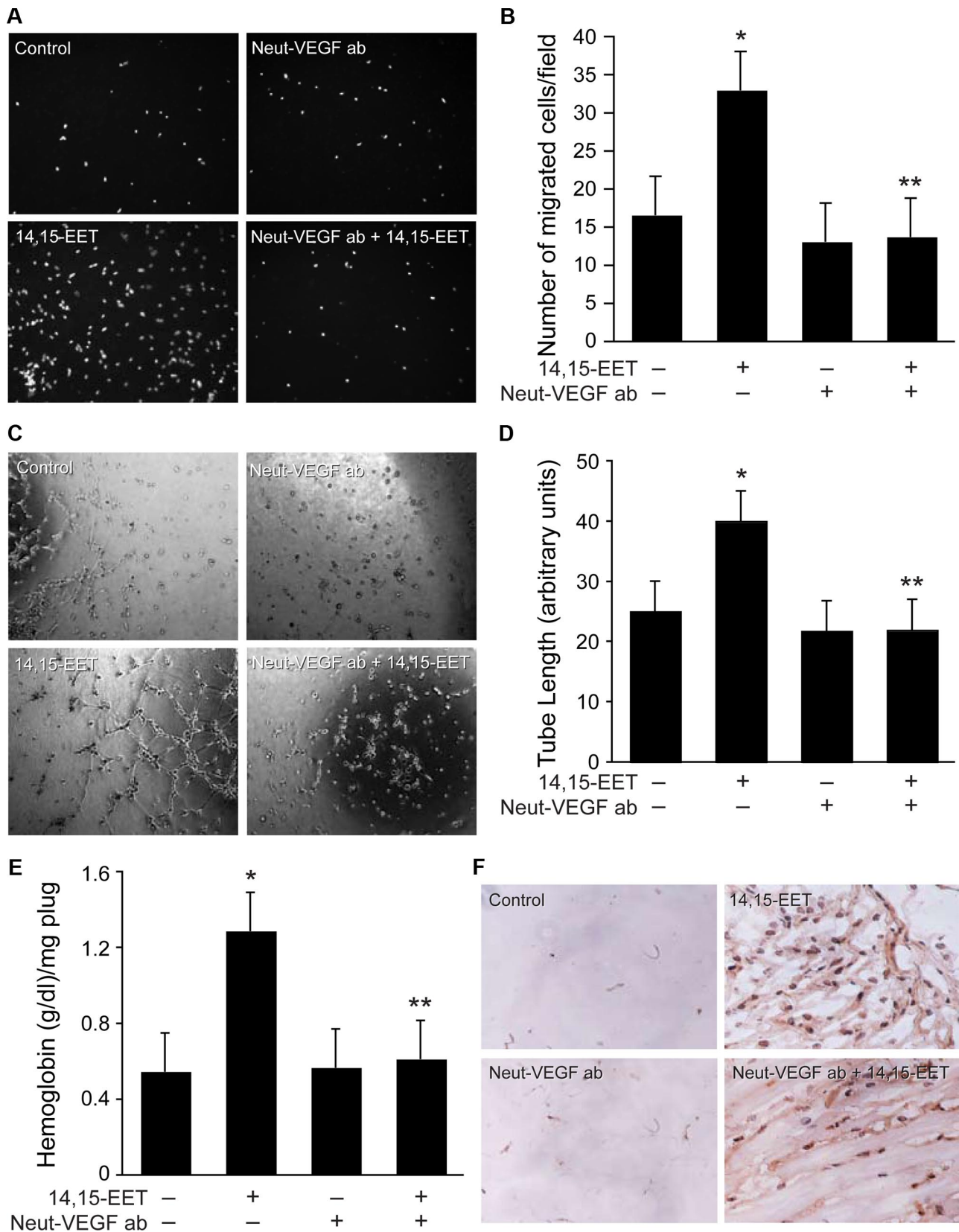
Figure 8. Neutralizing anti-VEGF antibodies suppress 14,15-EET–induced HDMVEC migration and tube formation in vitro and Matrigel plug angiogenesis in vivo. Quiescent HDMVECs were treated with neutralizing anti-VEGF antibodies (3 μg/mL) for 30 minutes at 37°C followed by washing with medium 131. The cells were then subjected to 14,15-EET (0.1 μM)–induced migration (A,B) or tube formation (C,D) in the presence and absence of 3 μg/mL neutralizing anti-VEGF antibodies. (E,F) C57BL/6 mice were injected subcutaneously with 0.5 mL Matrigel premixed with vehicle or 50 μM 14,15-EET with and without 3 μg/mL neutralizing anti-VEGF antibodies. One week later, the animals were killed and the Matrigel plugs were harvested from underneath the skin and analyzed for either hemoglobin content with Drabkin reagent or immunostained for CD31 expression using anti-CD31 antibodies. Preimmune serum was added to Ad-GFP– and Ad-GFP + 14,15-EET–treated cells or mice. The values in the bar graphs in panels B, D, and E are the means plus or minus SD of 3 independent experiments or 4 animals. *$P < .01$ vs control; **$P < .01$ vs 14,15-EET.
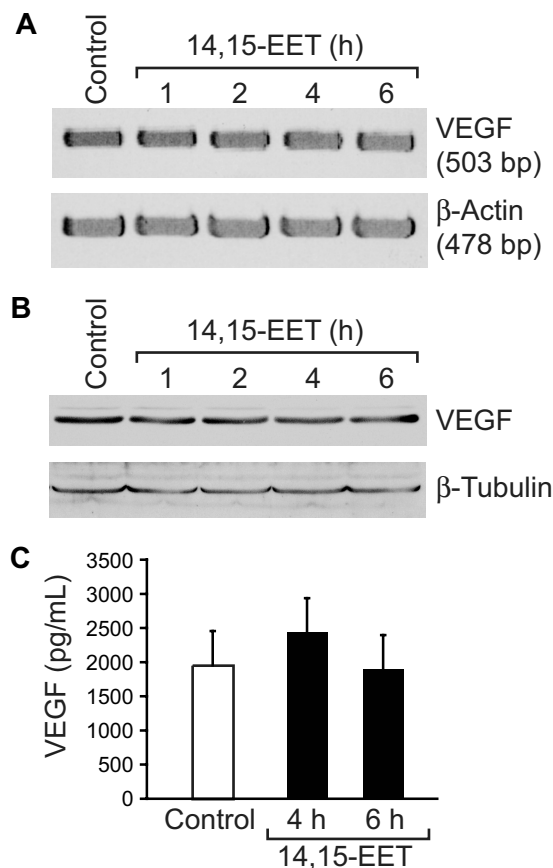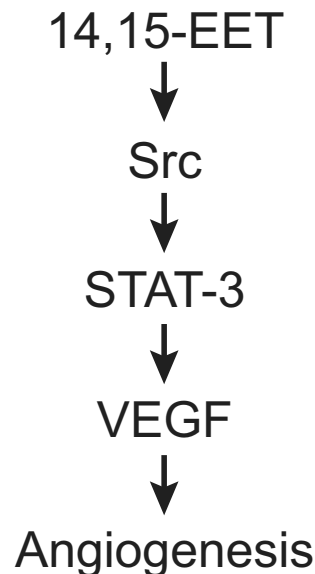
Figure 9. The lack of effect of 14,15-EET on VEGF expression in HASMCs. Quiescent HASMCs were treated with and without 14,15-EET (0.1 μM) for the indicated time periods and either RNA was isolated and analyzed for VEGF mRNA levels by RT-PCR (A), cell extracts were prepared and analyzed for VEGF protein levels by Western blotting (B), or the culture medium was collected and assayed for released VEGF by ELISA (C). Error bars represent SD.

Figure 10. Schematic diagram showing how 14,15-EET induces angiogenesis in HDMVECs.

angiogenesis. (3) 14,15-EET stimulated the tyrosine phosphorylation of Src, and blockade of its activation by adenovirus-mediated expression of its dominant negative mutant completely inhibited STAT-3 phosphorylation. (4) 14,15-EET induced the expression of VEGF in Src-STAT-3 activation signaling-dependent manner. (5) 14,15-EET also induced STAT-3 binding to VEGF promoter in vivo in a manner that is dependent on activation of Src-STAT-3 signaling. (6) Neutralizing anti-VEGF antibodies inhibited 14,15-EET–induced HDMVEC migration, tube formation, and Matrigel plug angiogenesis. Together, these findings reveal the capacity of 14,15-EET in the activation of Src-STAT-3 signaling leading to VEGF expression and angiogenesis.

STAT-3 plays a role in the regulation of cell proliferation, cell migration, and cell differentiation.[26-32,43,44] STAT-3 has also been shown to be involved in hypoxia-induced VEGF expression in pancreatic and prostate carcinomas.[45] Our results show that 14,15-EET activates STAT-3 in HDMVECs in an acute manner, which in turn, binds to VEGF promoter leading to its expression. Despite its labile nature, the capacity of 14,15-EET to activate STAT-3 at 1 bolus submicromolar concentration suggests for possible receptor activation in the propagation of its intracellular angiogenic signaling events. In this aspect, earlier studies have shown that EETs activate epidermal growth factor receptor (EGFR) in endothelial cells (ECs).[46] It was also demonstrated that stimulation of EGFR leads to activation of STAT-3.[47] In addition, some studies have shown that Src phosphorylates and activates EGFR.[48]

Since 14,15-EET stimulates Src and its blockade suppresses STAT-3 activation, it is likely that Src acts upstream to EGFR. It was also reported that stimulation of EGFR leads to activation of Src.[49] Therefore, Src could also act downstream to EGFR mediating STAT-3 activation by 14,15-EET. However, additional work is required to address whether 14,15-EET–stimulated Src-STAT-3 signaling requires the involvement of EGFR. 14,15-EET has been shown to activate Src in renal epithelial cells leading to their proliferation.[5] We have previously shown that 14,15-EET activates Akt via Src-dependent manner leading to FGF-2 expression and angiogenesis.[15] These findings lead to the speculation that Src plays a key role in mediating the intracellular signaling events of EETs, particularly of 14,15-EET. A role for Src in hypoxia-induced VEGF expression has also been demonstrated.[41] In this regard, it is interesting to point out that hypoxia induces CYP2C8/9 expression leading to increased production of EETs in ECs,[14] a finding that further suggests a role for these lipid molecules even in hypoxia-induced VEGF expression and angiogenesis. Based on these findings, it appears that Src-STAT-3 signaling plays a crucial role in the regulation of expression of VEGF in response to a wide variety of cues, including EETs.

Previously, we have shown that 14,15-EET–induced angiogenesis requires FGF-2.[15] In the present study, we report that VEGF mediates 14,15-EET–induced angiogenesis. Since inhibition of either FGF-2 or VEGF function via neutralizing antibody approach completely negated 14,15-EET–induced angiogenesis, it is likely that these growth factors are mediating stage-specific events of angiogenesis. As FGF-2 induction by 14,15-EET was found to be rapid compared with that of VEGF, the former may be involved in the initial stages of angiogenesis such as sprouting, whereas the latter molecule may be needed for survival and maintenance of the plasticity of the vessels. Such stage-specific roles for FGF-2 and VEGF have also been reported in the regulation of postnatal coronary angiogenesis, vascular development, and hypoxia and 2-fucosyl lactose (H-2g)–induced angiogenesis.[50-53] Regardless of their stage-specific roles, the induction of expression of both FGF-2 and VEGF is required for 14,15-EET–induced angiogenesis. Since 14,15-EET had no significant effects on VEGF expression in HASMCs,

a role for smooth muscle–dependent paracrine mechanisms, particularly via VEGF, is unlikely in the induction of angiogenesis by this lipid molecule. Many studies have reported that vasodilators such as adenosine stimulate angiogenesis.[54,55] A large body of data showed that EETs act as potent hyperpolarizing agents.[2,3] Similarly, the capacity of EETs in inducing angiogenesis has been demonstrated.[13-15] In this aspect, it is interesting to note that stressor conditions such as hypoxia that reduce the O_2 levels have been shown to induce the production of EETs.[4,16] The increased production of these lipid molecules under such stressor conditions may well be due to a geared protective response of the organ to reduced O_2 levels. Thus, while the actions of EETs on angiogenesis may be beneficial to tissues such as the ischemic heart, such effects may also aid in the development of diseases such as atherosclerosis, cancer metastasis, and tumor growth. It is now well established that hypoxia plays a central role in tumor growth.[56] Since hypoxia stimulates the production of EETs,[4,16] and EETs induce angiogenesis,[15-17] it is tempting to speculate a role for EETs in hypoxia-induced angiogenesis and tumor growth.

In summary, as depicted in schematic diagram shown in Figure 10, the present results provide the mechanistic insights of 14,15-EET–induced angiogenic events in HDMVECs, particularly the involvement of Src-STAT-3 signaling in mediating VEGF expression in HDMVECs, leading to their migration and tube formation and Matrigel plug angiogenesis.

Acknowledgment

Authorship

Contribution: S.Y.C. performed experiments on Western blot analysis, RT-PCR, ELISA, HDMVEC migration and tube formation, and Matrigel plug angiogenesis; M.K. performed experiments on RT-PCR, ELISA, EMSA, and ChIP assays; D.W. performed immunohistochemistry experiments; B.Z. performed experiments on isolation of nuclear and cytoplasmic extracts of HDMVECs and Western blot analysis; R.C.V. contributed critical reagents; G.N.R. designed experiments, interpreted the results, and wrote the paper.

Conflict-of-interest disclosure: The authors declare no competing financial interests.

Correspondence: Gadiparthi N. Rao, Department of Physiology, University of Tennessee Health Science Center, 894 Union Ave, Memphis, TN 38163; e-mail: grao@physio1.utmem.edu.

References

1. Spector AA, Norris AW. Action of epoxyeicosatrienoic acids on cellular function. Am J Physiol. 2007;289:C996-C1012.

2. Fisslthaler B, Popp R, Kiss L, et al. Cytochrome P4502C is an EDHF synthase in coronary arteries. Nature. 1999;401:493-497.

3. Campbell WB, Harder DR. Endothelium-derived hyperpolarizing factors and vascular cytochrome P450 metabolites of arachidonic acid in the regulation of tone. Circ Res. 1999;84:484-488.

4. Michaelis UR, Fisslthaler B, Barbosa-Sicard E, Falck JR, Fleming I, Busse R. Cytochrome P450 epoxygenases 2C8 and 2C9 are implicated in hypoxia-induced endothelial cell migration and angiogenesis. J Cell Sci. 2005;118:5489-5498.

5. Chen JK, Capdevila J, Harris RC. Over expression of C-terminal Src kinase blocks 14,15-epoxyeicosatrienoic acid-induced tyrosine phosphorylation and mitogenesis. J Biol Chem. 2000;275:13789-13792.

6. Potente M, Fisslthaler B, Busse R, Fleming I. 11,12-Epoxyeicosatrienoic acid-induced inhibition of FOXO factors promotes endothelial proliferation by down-regulating p27Kip1. J Biol Chem. 2003;278:29619-29625.

7. Node K, Huo Y, Ruan X, et al. Anti-inflammatory properties of cytochrome P450 epoxygenase-derived eicosanoids. Science. 1999;285:1276-1279.

8. Chen JK, Capdevila J, Harris RC. Cytochrome p450 epoxygenase metabolism of arachidonic acid inhibits apoptosis. Mol Cell Biol. 2001;21:6322-6331.

9. Dhanasekaran A, Al-Saghir R, Lopez B, et al. Protective effects of epoxyeicosatrienoic acids on human endothelial cells from the pulmonary and coronary vasculature. Am J Physiol. 2006;291:H517-H531.

10. Zeldin DC. Epoxygenase pathways of arachidonic acid metabolism. J Biol Chem. 2001;276:36059-36062.

11. Yu Z, Xu F, Huse LM, et al. Soluble epoxide hydrolase regulates hydrolysis of vasoactive epoxyeicosatrienoic acids. Circ Res. 2000;87:992-998.

12. Imig JD. Epoxide hydrolase and epoxygenase metabolites as therapeutic targets for renal diseases. Am J Physiol. 2005; 289:F496-F503.

13. Medhora M, Daniels J, Mundey K, et al. Epoxygenase-driven angiogenesis in human lung microvascular endothelial cells. Am J Physiol. 2003;284:H215-H224.

14. Pozzi A, Macias-Perez I, Abair T, et al. Characterization of 5,6- and 8,9-epoxyeicosatrienoic acids (5,6-EET and 8,9-EET) as potent in vivo angiogenic lipids. J Biol Chem. 2005;280:27138-27146.

15. Zhang B, Cao H, Rao GN. Fibroblast growth factor-2 is a downstream mediator of PI3K-Akt signaling in 14, 15-epoxyeicosatrienoic acid-induced angiogenesis. J Biol Chem. 2006;281:905-914.

16. Earley S, Pastuszyn A, Walker BR. Cytochrome P450 epoxygenase products contribute to attenuated vasoconstriction after chronic hypoxia. Am J Physiol. 2003;285:H127-H136.

17. Jiang JG, Ning YG, Chen C, et al. Cytochrome p450 epoxygenase promotes human cancer metastasis. Cancer Res. 2007;67:6665-6674.

18. Pozzi A, Ibanez MR, Gatica AE, et al. Peroxisomal proliferators-activated receptor-alpha-dependent inhibition of endothelial cell proliferation and tumorigenesis. J Biol Chem. 2007;282:17685-17695.

19. O'Brien ER, Garvin MR, Dev R, et al. Angiogenesis in human coronary atherosclerotic plaques. Am J Pathol. 1994;145:883-894.

20. Khurana R, Simons M, Martin JF, Zachary IC. Role of angiogenesis in cardiovascular disease: a critical appraisal. Circulation. 2005;112:1813-1824.

21. Folkman J. Angiogenesis in cancer, vascular, rheumatoid and other disease. Nat Med. 1995;1:27-31.

22. Davis GE, Senger DR. Endothelial extracellular matrix: biosynthesis, remodeling, and functions during vascular morphogenesis and neovessel stabilization. Circ Res. 2005;97:1093-1107.

23. Bromberg J, Darnell JE Jr. The role of STATs in transcriptional control and their impact on cellular function. Oncogene. 2000;19:2468-2473.

24. Cao H, Dronadula N, Rizvi F, et al. Novel role for STAT-5B in the regulation of Hsp27-FGF-2 axis facilitating thrombin-induced vascular smooth muscle cell growth and motility. Circ Res. 2006; 98:913-922.

25. Kundamani-Sridharan V, Wang D, Liu Z, Zhang C, Dronadula N, Rao GN. Activation of signal transducer and activator of transcription-5B in the vessel wall by balloon injury leads to cyclin D1 upregulation and neointima formation. Am J Pathol. 2007;171:1381-1394.

26. Wu YY, Bradshaw RA. Activation of the STAT3 signaling pathway is required for differentiation by interleukin-6 in PC12-E2 cells. J Biol Chem. 2000;275:2147-2156.

27. Jenkins BJ, Grail D, Nheu T, et al. Hyperactivation of STAT-3 in gp130 mutant mice promotes gastric hyperproliferation and desensitizes TGF-beta signaling. Nat Med. 2005;11:845-852.

28. Selander KS, Li L, Watson L, et al. Inhibition of gp130 signaling in breast cancer blocks constitutive activation of STAT-3 and inhibits in vivo malignancy. Cancer Res. 2004;64:6924-6933.

29. Hilfiker-Kleiner D, Hilfiker A, Fuchs M, et al. Signal transducer and activator of transcription 3 is required for myocardial capillary growth, control of interstitial matrix deposition, and heart protection from ischemic injury. Circ Res. 2004;95:187-195.

30. Neeli I, Liu Z, Dronadula N, Ma ZA, Rao GN. An essential role of Jak-2/STAT-3/cPLA2 axis in platelet-derived growth factor BB-induced vascular smooth muscle cell motility. J Biol Chem. 2004;279:46122-46128.

31. Wang D, Liu Z, Li Q, et al. An essential role for gp130 in neointima formation following balloon injury. Circ Res. 2007;100:807-816.

32. Srivastava K, Kundumani-Sridharan V, Zhang B, Bajpai AK, Rao GN. 15(S)-Hydroxyeicosatetraenoic acid-induced angiogenesis requires signal transducer and activator of transcription-3-dependent expression of vascular endothelial growth factor. Cancer Res. 2007;67:4328-4336.

33. Kilkenny DM, Rocheleau JV, Price J, Reich MB, Miller GG. C-Src regulation of fibroblast growth

factor-induced proliferation in murine embryonic fibroblasts. J Biol Chem. 2003;278:17448-17454.

34. Shah K, Vincent F. Divergent roles of c-Src in controlling platelet-derived growth factor-dependent signaling in fibroblasts. Mol Biol Cell. 2005;16:5418-5432.

35. Ishizawar R, Parsons SJ. C-Src and cooperating partners in human cancer. Cancer Cell. 2004;6: 209-214.

36. Fulton D, Church JE, Ruan L, et al. Src kinase activates endothelial nitric oxide synthase by phosphorylating Tyr-83. J Biol Chem. 2005;280: 35943-35952.

37. Nagata D, Mogi M, Walsh K. AMP-activated protein kinase (AMPK) signaling in endothelial cells is essential for angiogenesis in response to hypoxic stress. J Biol Chem. 2003;278:31000-31006.

38. National Center for Biotechnology Information. GenBank. http://www.ncbi.nlm.nih.gov/Genbank/index.html. Accessed August 2007.

39. Cao X, Tay A, Guy GR, Tan YH. Activation and association of Stat3 with Src in v-Src-transformed cell lines. Mol Cell Biol. 1996;16:1595-1603.

40. Silva CM. Role of STATs as downstream signal transducers in Src family kinase-mediated tumorigenesis. Oncogene. 2004;23:8017-8023.

41. Mukhopadhyay D, Tsiokas L, Zhou XM, Foster D, Brugge JS, Sukhatme VP. Hypoxic induction of human vascular endothelial growth factor expression through c-Src activation. Nature. 1995;375: 577-581.

42. Funamoto M, Fujio Y, Kunisada K, et al. Signal transducer and activator of transcription 3 is required for glycoprotein 130-mediated induction of vascular endothelial growth factor in cardiac myocytes. J Biol Chem. 2000;275:10561-10566.

43. Yahata Y, Shirakata Y, Tokumaru S, et al. Nuclear translocation of phosphorylated STAT3 is essential for vascular endothelial growth factor-induced human dermal microvascular endothelial cell migration and tube formation. J Biol Chem. 2003; 278:40026-40031.

44. Azare J, Leslie K, Al-Ahmadie H, et al. Constitutively activated Stat3 induces tumorigenesis and enhances cell motility of prostate epithelial cells through integrin beta 6. Mol Cell Biol. 2007;27: 4444-4453.

45. Gray MJ, Zhang J, Ellis LM, et al. Hif-1alpha, STAT3, CBP/p300 and Ref-1/APE are components of a transcriptional complex that regulates Src-dependent hypoxia-induced expression of VEGF in pancreatic and prostate carcinomas. Oncogene. 2005;24:3110-3120.

46. Michaelis UR, Fisslthaler B, Medhora M, Harder D, Fleming I, Busse R. Cytochrome P450 2C9-derived epoxyeicosatrienoic acids induce angiogenesis via cross-talk with the epidermal growth factor receptor (EGFR). FASEB J. 2003;17:770-772.

47. Grandis JR, Drenning SD, Chakraborty A, et al. Requirement of Stat3 but not Stat1 activation for epidermal growth factor receptor-mediated cell growth in vitro. J Clin Invest. 1998;102:1385-1392.

48. Sato K, Nagao T, Iwasaki T, Nishihira Y, Fukami Y.

Src-dependent phosphorylation of the EGF receptor Tyr-845 mediates Stat-p21waf1 pathway in A431 cells. Genes Cells. 2003;8:995-1003.

49. Murillo MM, del Castillo G, Sánchez A, Fernández M, Fabregat I. Involvement of EGF receptor and c-Src in the survival signals induced by TGF-beta1 in hepatocytes. Oncogene. 2005; 24:4580-4587.

50. Tomanek RJ, Sandra A, Zheng W, Brock T, Bjercke RJ, Holiield JS. Vascular endothelial growth factor and basic fibroblast growth factor differentially modulate early postnatal coronary angiogenesis. Circ Res. 2001;88:1135-1141.

51. Poole TJ, Finkelstein EB, Cox CM. The role of FGF and VEGF in angioblast induction and migration during vascular development. Dev Dyn. 2001;220:1-17.

52. Calvani M, Rapisarda A, Uranchimeg B, Shoemaker RH, Melillo G. Hypoxic induction of an HIF-1alpha-dependent bFGF autocrine loop drives angiogenesis in human endothelial cells. Blood. 2006;107:2705-2712.

53. Zhu K, Amin MA, Zha Y, Harlow LA, Koch AE. Mechanism by which H-2g, a glucose analog of blood group H antigen, mediates angiogenesis. Blood. 2005;105:2343-2349.

54. Clark AN, Youkey R, Liu X, et al. Circ Res. 2007; 101:1130-1138.

55. Adair TH. Growth regulation of the vascular system: an emerging role for adenosine. Am J Physiol. 2005;289:R283-R296.

56. Keith B, Simon MC. Hypoxia-inducible factors, stem cells, and cancer. Cell. 2007;129:465-472.